Report for BAA Jupiter Section web page

Jupiter's polar polygons: Circumpolar clusters of cyclones: ADDENDUM

This Addendum gives full details of our measurements of internal rotation of the cyclones, made in 2017 March. The results are presented here following improved calculations. CPCs are numbered as in Adriani et al.(2018, Nature).
–John Rogers (2018 Dec.28).

Circulations of the CPCs

Methods:
The circulations in these cyclones are fast enough (0.1 to 0.3 deg/min) that they can be measured from images taken only 15-30 min apart. The measurements were performed by JHR on Gerald Eichstädt's polar projection maps of individual images, slightly adjusted to optimise alignment by reference to the large-scale features such as CPCs, then superimposed and 'blinked' to reveal the rotations. For each pole, I used two maps at PJ1, three maps at PJ3, and two maps at PJ4.

Within each CPC, angular velocities about the apparent centre were measured in concentric annuli (from one to six per CPC) (e.g. Figure N6). To measure the angular displacement, the annulus in one image was rotated on screen until it appeared registered with its equivalent in the other image. Each annulus was chosen so as to include sufficient features to give a definite angular velocity that was different from adjacent annuli. The stated angular velocity is the consensus for the more distinct features in the annulus, and the 'error' represents the range of values which appear reasonable, or the average of measurements between multiple pairs of images; sometimes there were minor features with slightly different speeds. Uncertainties are present due to real local motions, and also image noise, residual misalignments of maps, and uncertainty in locating the exact center of the CPC. Image processing was done in Adobe Photoshop Elements, and calculations and charts were made in Microsoft Excel. I assume that 1 degree latitude = 1167 km.

Although a single angular velocity is given for each annulus, this is undoubtedly an oversimplification. The results are consistent with a smooth trend of angular velocity with radius, subject to the local deviations mentioned above.

Results:
Using polar projection maps from the PJ1, PJ3 and PJ4 images, the angular velocities were measured in concentric annuli in the best-resolved CPCs. Different classes were analysed separately: southern CPCs, filled northern CPCs, and chaotic northern CPCs.

In every case for which more than one annulus could be measured, the angular velocity increased with decreasing radius, except in the inner bright cloud deck of the northern filled CPCs. The angular velocities are plotted against radius in Fig. N7. It is evident that most of the CPCs within all of the three classes fall close to a single curve, although some points for chaotic northern CPCs are lower. The rotation curves are approximately exponential; as shown in Fig.N7C, the values for each of the three classes are well fitted by straight lines when the log of the angular velocity is plotted. The southern CPCs have a regression line indistinguishable

from that of the northern filled CPCs. The northern chaotic CPCs follow a slower regression line but with more scatter.

The inner limit of measurable rotation in most cases was r ~ 600-900 km. Closer to the centre:
(i) For the southern CPCs: Speeds in some examples (including the central one) were still increasing down to r < 750 km, with rotation visible down to r < 400 km. The highest angular velocity was for the smallest radius that we measured, in the centre of CPC-s1 at PJ3, 0.53 (±0.024) deg/min, giving an implied rotation period of 11.3 hours.
(ii) For the northern 'chaotic' CPCs, one example showed angular velocity increasing down to very small radius.
(iii) For the northern 'filled' CPCs, the inner bright part did not show a centrally increasing angular velocity: two out of three examples showed a uniform rotation rate over a large span from the edge of the inner bright part inwards. Indeed, in the largest ones there were signs of inner spiral structure suggesting that the very center rotated less strongly or even, as observed in at least one case, in the opposite direction (see below).

The derived wind speeds are plotted against radius in Fig. N8. Despite the large scatter overall, the wind speeds have consistent trends with radius, best seen by examining individual CPCs (Fig.N8B,C). Lines are drawn between points representing the same CPC, and substantial differences between individual CPCs are evident. Nevertheless, all have speeds increasing with decreasing radius in the outer parts, typically at a rate of ~-3.2 to -5.7 m/s/100km (-3.2 to -5.7 $x10^{-5}$ s^{-1}). Apart from the South Polar Cyclone (SPC, the central one), all have peak speed of 64-99 m/s at ~900 < r < 1600 km. The SPC at PJ3 had the highest wind speeds that we recorded: the central oval had an angular velocity of 0.515 (±0. 033) deg/min, giving a mean speed of 100.5 (±6.4) m/s, and an implied rotation period of 11.6 hours. The wind speed amounted to ~130 m/s at the outer ends of the oval. [These values supercede those given in the main report.] However at PJ1 and PJ4 the central rotation was more modest and the SPC's rotation curve in general was similar to other CPCs.

For the wind speed gradient near the very centre of the CPCs, where we find no trackable features, we can only give lower limits, by assuming that wind speed declines linearly from the middle of the innermost measured annulus to the centre. Taking those CPCs where rotation was tracked to r < 1000 km, we find minimum gradients ranging from 5.0-9.2 m/s/100km for 6 northern CPCs, and 6.6-15.4 m/s/100km for southern CPCs-s1, -s4, & the SPC.

In two of the northern filled CPCs at PJ1, within the central bright cloud deck there were spiral streaks in opposite sense to those in the periphery (e.g. Fig. N5), suggesting that the centre was rotating less rapidly than the peripheral part, or even in the opposite direction. These regions could not be measured. On one occasion (CPC-n5 at PJ6), Gerald's animation showed that the central region was definitely rotating anticyclonically, opposite to the rest of the cyclone.

Measurement of FFRs:
For comparison with the CPCs, I measured one large FFR (folded filamentary region; cyclonic) and three 'mini-FFRs' at slightly lower latitudes than the CPCs. The 'mini-FFRs' were oval cyclonic features resembling the bright central cores of some northern filled CPCs; the measurements showed them to have a range of angular velocities and wind speeds, generally slower than the CPCs.
For the large FFR (south of CPC-n1 at PJ3), because its circulation was obviously not circular, I measured linear displacements over 3 images. The deduced wind speeds were similar along the north, south and east edges; combining them gave a mean speed of 60.1 m/s (±8.8 m/s, SD;

n=9). Inside the FFR, the wind speeds were less, and near zero close to the central axis. As the north-south span was ~2300 km, the mean wind speed gradient was 5.2 m/s/100km. This compares with a mean gradient of ~1.9 m/s/100km for a large FFR or turbulent segment of the South Temperate Belt [MJ & SL, 2002; Icarus 160, 325; their Figs.3 & 4], which is also typical of Jupiter's larger belts in general.

Surrounding structures and circulation

In the south polar region, at each perijove there are several small anticyclonic white ovals scattered outside the pentagon, and we suspect that some of these can be tracked from PJ1 to PJ6, drifting eastwards around the perimeter of the pentagon, in line with the circulations of the CPCs, but at slow and irregular speeds. Fig. N9 shows the proposed identifications and drifts.

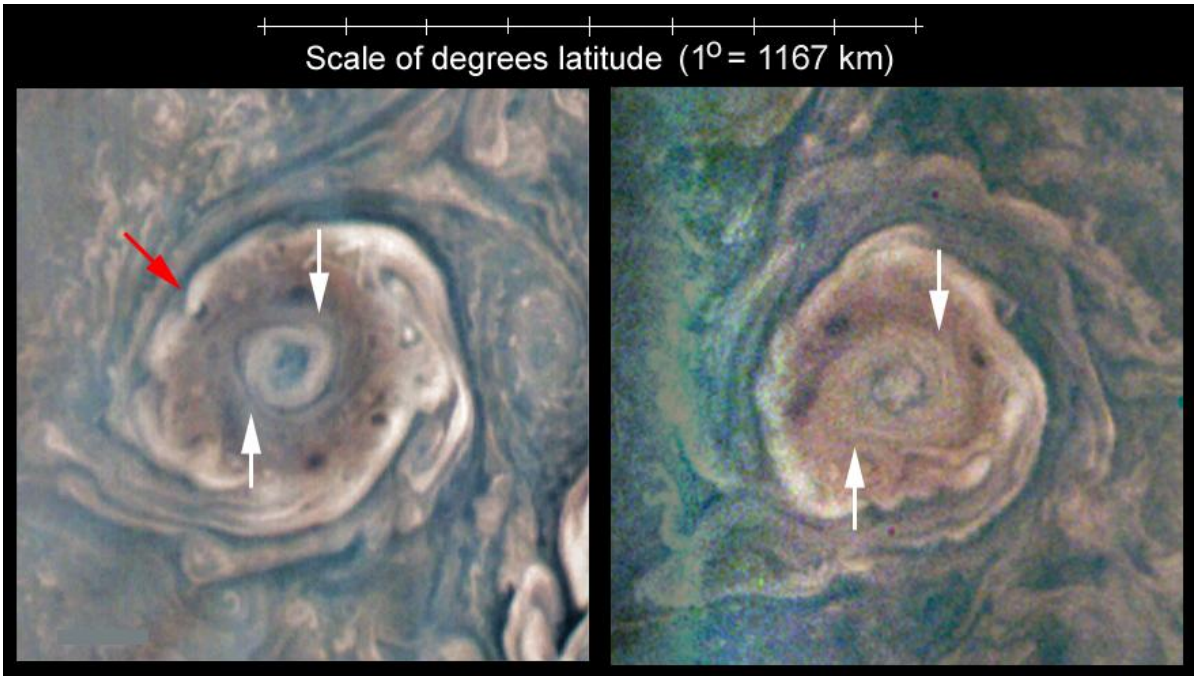

Figure N5:
High-resolution views of the largest northern filled CPC, showing counter-spiral structure near the centre.
Left, PJ1; right, PJ6.
(At PJ6, animation of these images showed counter-rotation in the centre.)
Credit: NASA / SwRI / MSSS / Gerald Eichstädt / John Rogers.

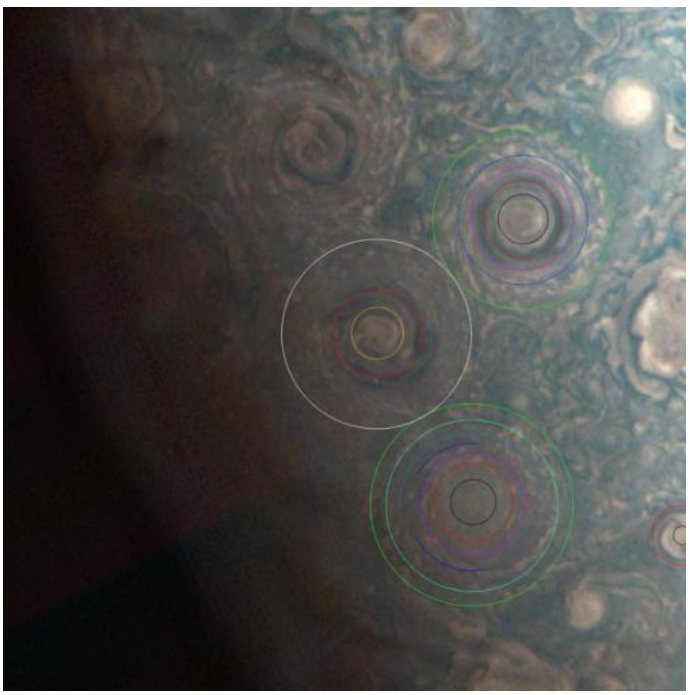

Figure N6 (right).
Example of a map-projected images with annuli marked on selected CPCs for angular velocity measurement.
(PJ1, South pole)
Credit: NASA / SwRI / MSSS / Gerald Eichstädt / John Rogers.

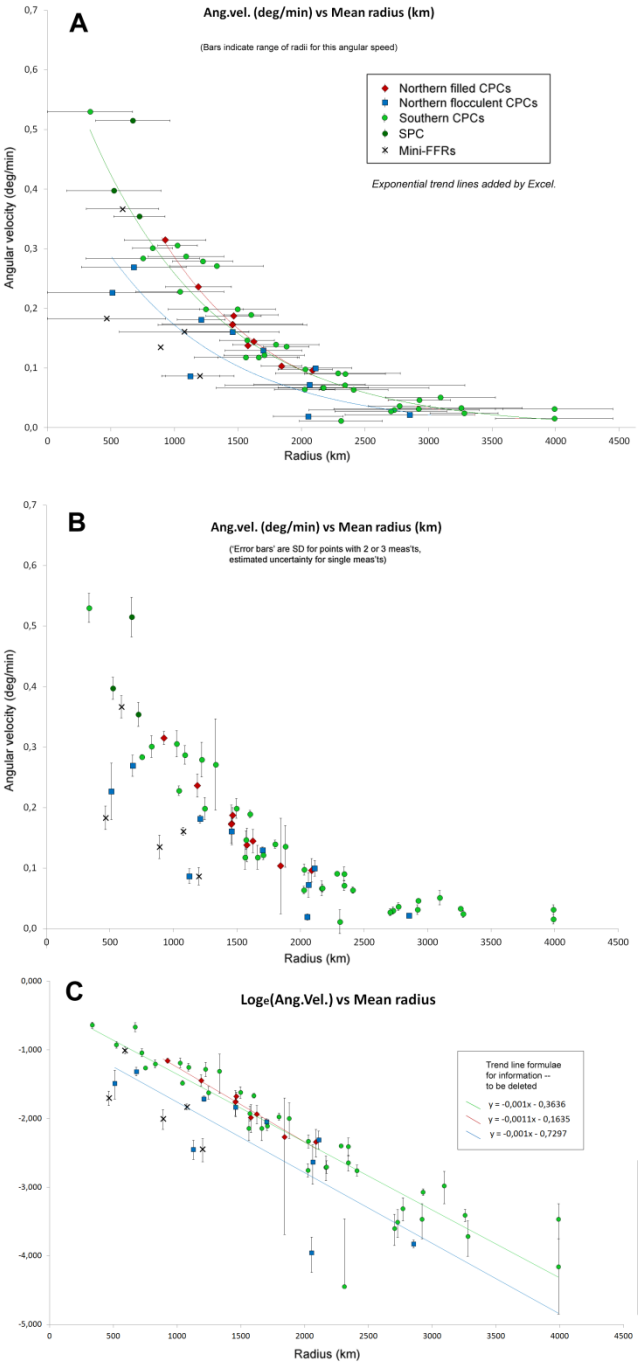

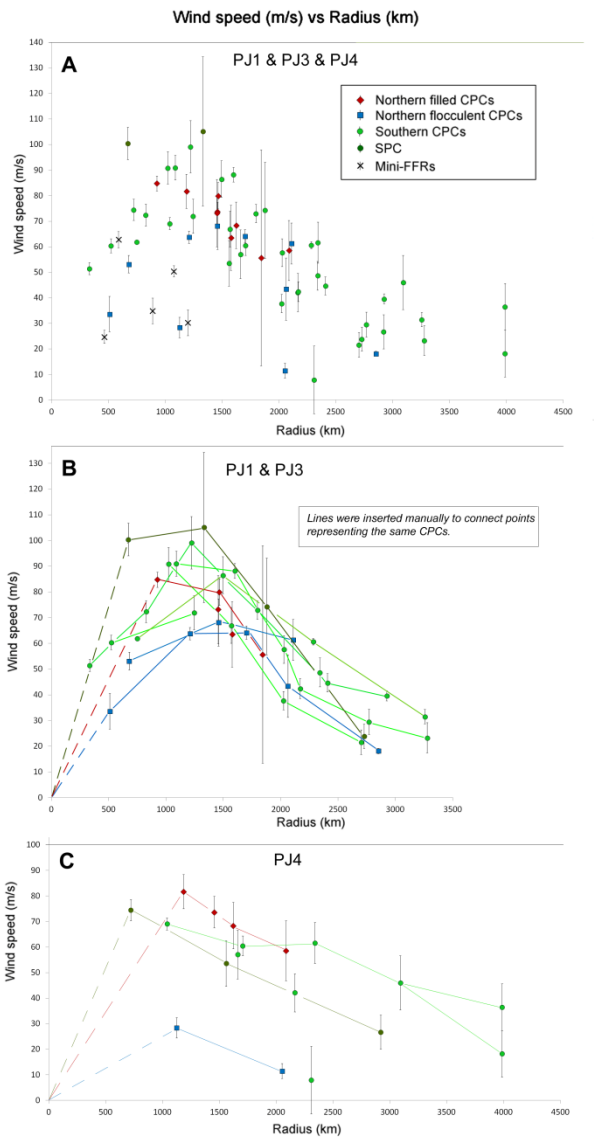

Figure N7 (left). Angular velocities within the CPCs, plotted against radius from the centre of each CPC. (A) All data with radial extents of annuli, and with separate logarithmic fits to the 3 classes of CPCs. (B) The same data with error bars for angular velocities. (C) The same data plotted as the natural logarithm of the angular velocity.

Figure N8 (right). Tangential wind speeds within the CPCs, calculated from the data in Fig.N7. (A) All data. (B,C) Data for separate perijoves; individual CPCs are connected by lines.

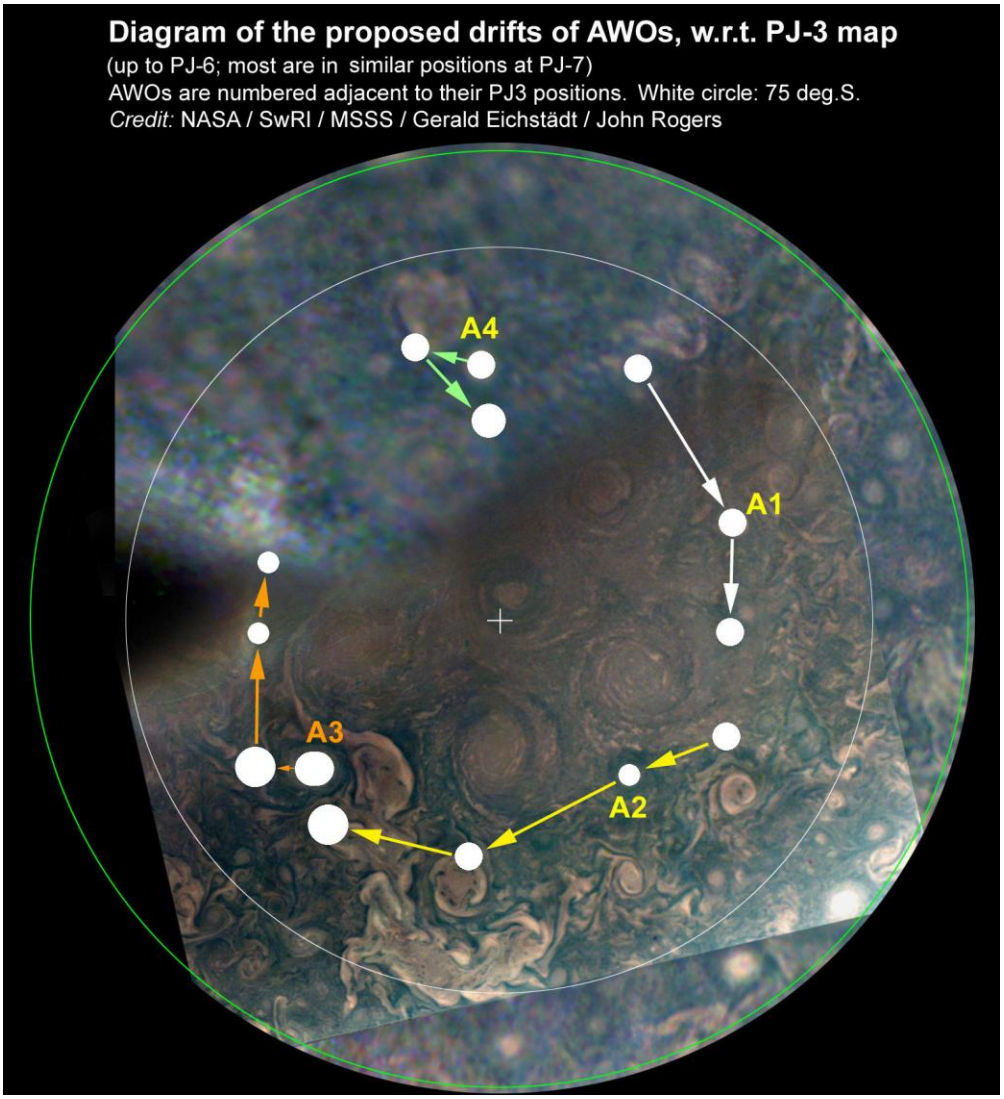

Figure N9. Tentative tracking of small anticyclonic white ovals around the perimeter of the south polar pentagon from PJ1 to PJ6. (Most were in similar positions at PJ7.) They are plotted relative to the pentagon (not relative to the pole), on a preliminary PJ3 polar projection map, with L3=0 to the left.